EVALUACIÓN CUANTITATIVA DE LA CALIDAD DE IMAGEN EN TC DE TÓRAX: RESULTADOS PRELIMINARES—UN NUEVO ENFOQUE A PROBLEMAS ANTIGUOS

QUANTITATIVE EVALUATION OF THORAX CT IMAGE QUALITY: PRELIMINARY RESULTS—A NEW APPROACH TO OLD PROBLEMS

A. López*[1], J. Reyes[2], J.L. Delgado[3], C. Ubeda[4], C.F. Calderón[5], J.J. González[5] y L.A. Torres[6]

[1]*Departamento de Ciencias Físicas, Centro de Física e Ingeniería en Salud (CFIS), Universidad de La Frontera, Avenida Francisco Salazar 01145, Temuco 4811230, Región de La Araucanía, Chile*

[2]*Instituto Superior de Tecnologías y Ciencias Aplicadas (InSTEC) — Universidad de La Habana, Avenida Salvador Allende #1110, Plaza de la Revolución, La Habana 10400, Cuba*

[3]*Universidad Agraria de La Habana "Fructuoso Rodríguez Pérez" (UNAH), Autopista Nacional km 23 1/2 y Carretera de Tapaste, San José de las Lajas 32700, Provincia Mayabeque, Cuba*

[4]*Departamento de Tecnología Médica — Facultad de Ciencias de la Salud. Universidad de Tarapacá Avenida 18 de Septiembre #2222, Campus Saucache, Arica 1000000, Chile*

[5]*Instituto Nacional de Oncología y Radiobiología (INOR), Calle 29 esquina F, Vedado, Plaza de la Revolución, La Habana 10400, Cuba*

[6]*Departamento de Servicios Biomédicos. Centro de Isótopos (CENTIS)Avenida Monumental y Carretera La Rada, km 3 1/2, San José de las Lajas 32700, Provincia Mayabeque, Cuba*

Recibido: 22/06/2025 ; Aceptado: 19/01/2026

La optimización de las dosis en Tomografía Computada es tema de constante investigación, incluyendo la búsqueda de métricas objetivas de calidad de imagen especialmente en escenario clínico. Este trabajo evaluó la capacidad de nuevas métricas de calidad de imagen para distinguir entre protocolos de tomografía computarizada (TC) de tórax de Baja Dosis y Diagnóstico en los mismos pacientes. Se analizaron 30 estudios clínicos correspondientes a 15 pacientes (un estudio por protocolo en cada caso). Las métricas consideradas fueron la relación contraste-ruido en escenario clínico (CNRc) y su promedio (CNRca), así como la resolución espacial clínica obtenida como ancho total a la mitad del máximo (FWHMc) y su valor medio por imagen (FWHMca), estimados a partir de la función de dispersión del borde de estructuras anatómicas relevantes. Los tamaños de dosis específicos (SSDE) fueron 8,8 $\pm$ 1,5 mGy para Baja Dosis y 13,5 $\pm$ 2,9 mGy para Diagnóstico. El CNRc y el FWHMca evidenciaron diferencias estadísticamente significativas entre protocolos: el FWHMca varió de 1,40–1,97 mm en Baja Dosis frente a 0,9–1,2 mm en Diagnóstico. Estos resultados confirman que CNRc, FWHMc y, en especial, FWHMca permiten caracterizar cuantitativamente la calidad clínica de la imagen, aunque se requieren estudios ampliados para consolidar estas observaciones.

Palabras Clave: calidad de imagen clínica, TC, métrica de calidad.

The optimization of dose in Computed Tomography is a topic of ongoing research, including the search for objective image-quality metrics, especially in the clinical setting. This study evaluated the ability of new image-quality metrics to discriminate between Low-Dose and Diagnostic chest CT protocols in the same patients. Thirty clinical examinations corresponding to 15 patients were analyzed (one study per protocol for each patient). The metrics considered were the clinical contrast-to-noise ratio (CNRc) and its mean value (CNRca), as well as the clinical spatial resolution expressed as the full width at half maximum (FWHMc) and its mean value per image (FWHMca), estimated from the edge-spread function of relevant anatomical structures. Size-specific dose estimates (SSDE) were 8.8 $\pm$ 1.5 mGy for the Low-Dose protocol and 13.5 $\pm$ 2.9 mGy for the Diagnostic protocol. CNRc and FWHMca exhibited statistically significant differences between protocols: FWHMca ranged from 1.40–1.97 mm in Low-Dose scans versus 0.9–1.2 mm in Diagnostic scans. These results confirm that CNRc, FWHMc and, in particular, FWHMca can quantitatively characterize clinical image quality, although larger-scale studies are needed to consolidate these observations.

Keywords: clinical image quality, CT, quality metric.

https://doi.org/10.31527/analesafa.2026.37.1.6-12 ISSN - 1850-1168 (online)

I. INTRODUCTION

Since Sir Godfrey Hounsfield introduced the first computed tomography (CT) scanner in 1972, both the application and clinical value of the technique have expanded steadily. According to the United Nations Scientific Committee on the Effects of Atomic Radiation (UNSCEAR), CT examinations now account for 61.6 % of the collective effective dose per capita, and the global volume of CT studies has risen by roughly 80 % over the last decade [1]. Recent investigations also highlight the cumulative radiation burden from repea-

* adlin.lopez@ufrontera.cl

ted CT imaging: in many patients, the sum of doses from diagnostic CT procedures often exceeds 100 mSv, markedly increasing the probability of radiation-induced effects [2, 3]. This evidence demands the need to optimize exposure in terms of reducing radiation doses without affecting the quality of the images that it should provide. The introduction of new scientific advances in different areas ranging from technological developments related to equipment design, to image reconstruction and processing methods, constitute aspects of continuous research [4-6]. The relationship between radiation dose and image quality is complex. It cannot always be described or evaluated using phantoms because it depends on the clinical objective and the study subject's diagnostic needs and habitus. Added to this is the subjective component of the observer-based image quality assessment, which is radiologist-dependent as he is the ultimate arbiter of image quality at presentation and can show significant intra- and inter-observer variability [5, 7, 8]. For this reason, finding image quality metrics that are adapted to the specific clinical scenario can help to objectively assess image quality and correlate it with dose, and can facilitate data-driven image quality and dose monitoring for the purpose of optimizing [9-11]. This study is designed as a proof-of-concept to demonstrate the clinical utility of image quality metrics that have already shown sensitivity to protocol and dose related variations. López et al. reported a statistically significant correlation between dose indicators in 20 chest CT examinations acquired with different protocols [12], using as primary metrics the contrast-to-noise ratio between adjacent structures (CNRc) [13]; the clinical spatial resolution expressed as the full width at half-maximum (FWHM) derived from the anatomical edge-spread function; and the mean FWHM value per image (FWHMca). The FWHM defined through this methodology was introduced by Almahdi et al. under phantom conditions [14] and later extended to the clinical setting by López et al. [12]. Building on this experience, the present work aims to verify by analysing two chest CT studies of the same patient acquired with protocols of different diagnostic quality whether these metrics can discriminate the resulting image quality differences, thereby supporting their potential routine application in clinical practice.

II. METHODS

A Retrospective Case Series Study [15] was conducted from September 2021 to October 2022, selecting 30 studies, from 15 adult oncologic patients who underwent two studies under different acquisition and processing protocols: one Low Dose with localization and attenuation correction purposes and one for Diagnostic purposes. To introduce and evaluate those quantitative parameters to objectively study the quality of the chest CT image, 30 studies were analysed. The studies were stored in the National Institute of Oncology and Radiobiology (INOR) dataset, Havana, Cuba, and were performed over a maximum of 6 months between protocols. The equipment used was the PET/CT Philips Gemini 64TF hybrid equipment [16]. Table 1 describes the patients' general characteristics and both protocols.

The CaDICT tool developed in MATLAB 2008b was used for image analysis and processing [12, 17]. The related dosimetry parameters were obtained, which in this case were volumetric CT dose index (CTDIvol in mGy) [18] and Size-Specific Dose Estimates (SSDE, in mGy) [19].

The quality metrics evaluated were the CNRc and its average value CNRca, according to expression (1); the clinical spatial resolution by pairs of structures FWHMc, obtained from the edge spread function between important anatomical structures of the thorax such as the heart (C), liver (H), left and right lung (PI and PD), right and left muscle of the back (MDE and MIE), right muscle and left muscle of the chest (MDP and MIP); using expression (2) [9, 13, 20]. The rationale for using various tissues is related to describing the clinical problem with the selected metrics, closely related to the clinical scenario. The average value of this parameter per image (FWHMca) was also obtained as a way to characterize the clinical spatial resolution globally [12]. See an example of how these edge profiles were obtained in Figure 1.

Parameter	Male (40%)		Female (60%)	
	Average ± SD*	Range*	Average ± SD*	Range*
Age (years)	63 ± 16	37–79	62 ± 11	47–78
Body weight (kg)	73 ± 18	51–93	67 ± 9	54–85
Height (m)	1.8 ± 0.1	1.6–1.9	1.6 ± 0.1	1.6–1.7
	Low dose		Diagnostic	
kV	120		120 ± 5	120–140
Nominal mAs	100		230 ± 43	148–290
mAs	100		15 ± 38	97–229
Slice thickness (mm)	5		3	
Pitch	0.9 ± 0.1	0.8–1.12	1.1 ± 0.1	1.0–1.2
Convolution kernel	B		3C 1YB 11B	

*Expressed when it is possible

TABLA 1: General characteristics of the patients and CT protocols.

The contrast to noise ratio (CNRc) of tissues or organs is obtained under the expression:

$$CNRc = \frac{(MPV_{organ} - MPV_{background})}{\sqrt{\frac{SD^2_{organ} + SD^2_{background}}{2}}} \quad (1)$$

Where:

MPV_{organ}: mean value per pixel of CT number determined from a Region of Interest (ROI) performed on the organ or tissue of interest.

$MPV_{background}$: mean value per pixel of the number of CT found from an ROI performed on the tissue or organ surrounding the structure.

SD: Standard deviation of the number of CT corresponding to the ROI performed on the structure/organ and the background.

The edge spread function (ESF) is obtained by fitting the obtained profiles to the following equation 12,14:

$$ESF = \frac{1}{2} + \frac{1}{\pi} tan^{-1}(\lambda(x - x_0)) \quad (2)$$

Where: λ and x_0 are the adjustment parameters, and the FWHMc= $2/\lambda$ expressed in mm.

For the statistical analysis of the results, the IBM SPSS Statistics 20 program (User's Manual) was used21. The numerical variables studied (CNRc, CNRca, FWHMc,

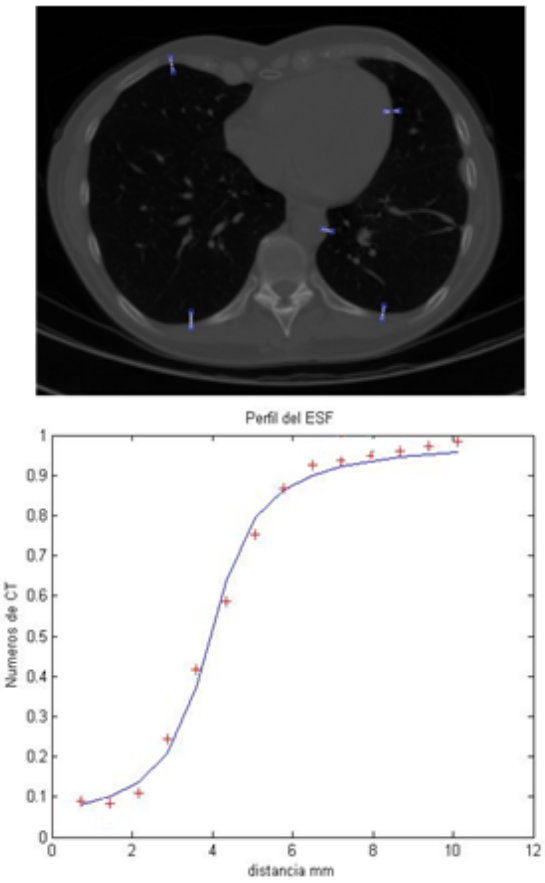

FIG. 1: Example that illustrates the process of obtaining the edge spread functions (ESF), a) Example of edge profiles drawn on the image, b) Example of one profile.

FWHMca, CTDIvol, SSDE) were analysed using the Wilcoxon signed-rank test (nonparametric, paired) with 95% confidence level and p<0.05 statistical significance.

The Pearson correlation test was used with a 95% confidence level and p<0.05 of statistical significance to study the possible relationship of the image quality metrics with the dosimetry parameters.

III. RESULTS

The results of the dosimetry parameters per patient for each protocol are summarised in Table 2, including the mean values, median, standard deviation, and the statistical significance of their comparison.

Table 3 shows the average, maximum, and minimum values of the CNRc per type of study in each of the selected structures, the statistical significance (p) between protocols, and the average Contrast to Noise Ratio (CNRca) for each study.

Figure 2 presents the CNRc absolute differences between Low Dose and Diagnostic protocols in different pairs of organs, per patient, meanwhile, Figure 3 shows the average values of the edge spread function (FWHMca) per patient for each protocol.

Table 4 shows the average FWHMc values per structure for the low-dose and diagnostic studies, as well as the p-values found during their statistical comparison

.

TABLA 2: Dosimetry parameters per patient.

	CTDIvol (mGy)		SSDE (mGy)	
Patients	Low Dose	Diag.	Low Dose	Diag.
P1	5.9	10.6	8.9	15.4
P2	5.9	10.5	8.3	13.9
P3	5.9	11.5	6.8	12.2
P4	5.9	15.4	7.9	20.4
P5	5.9	7.4	9.8	13.8
P6	5.9	10.1	9.7	17.2
P7	5.9	6.7	11.7	11.1
P8	5.9	6.8	7.6	10.2
P9	5.9	8.8	9.4	13.9
P10	5.9	5.7	9.3	8.9
P11	5.9	6.6	8.7	10.3
P12	5.9	9.9	6.9	12.5
P13	5.9	9.9	10.0	15.0
P14	5.9	9.0	10.0	14.5
P15	5.9	11.9	6.5	13.6
Average	5.9	9.4	8.8	13.5
Median	5.9	9.6	8.8	13.7
SD	0.00	2.5	1.5	2.9
p	0.001		0.005	

SD- Standard deviation, Diag.-Diagnostic

TABLA 3: Description of CNRc per type of study and the Average Contrast to Noise Ratio (CNRca).

	CNRc			
	H-PD		**MDE-PD**	
	Low Dose	Diagnostic	Low Dose	Diagnostic
p	0.003	0.003		
Maximum	29.7	47.8	29	50.0
Minimum	8.2	11.8	8.3	11.7
CNRca	14.2	29.3	13.6	29.0
SDca	5.5	13.9	5.3	14.8
SD (%)	38.7	47.4	39.1	51.0
	CNRc			
	H-PD		**MDE-PD**	
	Low Dose	Diagnostic	Low Dose	Diagnostic
p	0.015	0.023		
Maximum	58.5	116.2	75.2	136.5
Minimum	12.2	18.6	12.3	21.8
CNRca	35.5	59.8	42.0	65.4
SDca	13.9	23.9	18.3	27.6
SD (%)	39.2	40.0	43.5	42.2

IV. DISCUSSION

According to Table 2, CTDIvol values ranged from 5.7 to 15.4 mGy, showing average values of 9.4±2.6mGy for Diagnostic protocol, while for Low Dose studies it was 5.9 mGy, showing significant differences (p=0.001). The values obtained for the SSDE range from 6.5 to 11.7mGy with an average of 8.8±1.5 mGy for the Low Dose studies. For the Diagnostic studies the average values are 13.5±2.9 mGy, and the same values are in the range 8.9-20.4mGy, showing significant differences between both protocols (p=0.001). The differences obtained between SSDE and CTDIvol were significant (p=0.001), in all cases SSDE was higher than

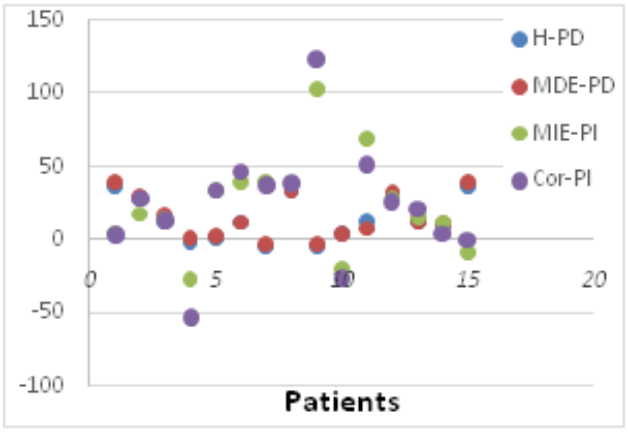

FIG. 2: Absolute Differences in CNRc between Low Dose and Diagnostic protocols, for different pairs of organs, per patient.

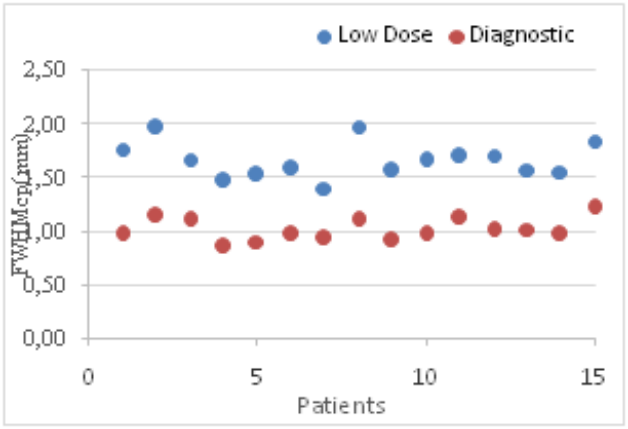

FIG. 3: FWHMcp values per patient for each protocol

CTDIvol, resulting in a higher patient dose than the estimated reference, consistent with other authors' findings [12, 21, 22] . In both cases, the average values of the dosimetry magnitudes were comparable to diagnostic reference values reported for those study types [23, 24].

Table 3 shows that CNRc results for the selected adjacent structures showed a wide range of variation between structures and protocols. It ranged for low doses between 8.6 and 42, while for Diagnostic they ranged between 29.3 and 65. Mainly, the Diagnostic protocols showed higher CNRc values for the same structures as shown in Figure 3. The CNRc of the Liver-Right Lung and Back Muscle-Right Lung, yielded mean values lower than 15 (14.2 and 13.6) for Low Dose and lower than 30 (29.3 and 29.0) for Diagnostic studies, while the rest of the CNRc showed higher values. The differences observed between both protocols for each CNRc were significant ($p \leq 0.023$). This task-oriented indicator (CNRc) is calculated using different equations in the literature, and therefore, varies widely in magnitude [25]. It was originally defined in quality control phantoms (where the background is of uniform material and usually a single region), and for its application to clinical tasks, some authors report a definition of noise associated with a single anatomical structure, which varies with each author's report, as well as their results [26-28].

Heart (C), liver (HB), left and right lung (PI and PD), right and left muscle of the back (MDE and MIE), right muscle and left muscle of the chest (MDP and MIP). Diag-Diagnostic, LD-Low Dose

TABLA 4: $FWHM_c$ average, minimum, and maximum values per study type

	Aorta-PI		**MIE-Soft tissue**	
	LD	Diag.	LD	Diag.
p	0.002		0.001	
Maximum	2.2	1.3	2.7	1.5
Minimum	0.9	0.7	1.0	0.7
Average	1.4	0.9	1.7	1.1
SD	0.4	0.2	0.4	0.2
SD (%)	26.7	20.9	25.8	19.7
	MIE-PI		**C-PI**	
	LD	Diag.	LD	Diag.
p	0.001		0.001	
Maximum	2.4	1.4	2.6	1.5
Minimum	1.1	0.8	1.1	0.8
Average	1.7	1.0	1.7	1.0
SD	0.4	0.2	0.5	0.2
SD (%)	21.1	16.6	28.6	20.5

In the previous study developed by this author, low CNRc values were reported for non-contiguous structures, Aorta/Soft Tissue 2.9 (1.0-5.5) and Heart/Soft Tissue 2.8 (0.9-5.3). In contiguous structures CNRc showed high values of noise contrast ratio (CNRc>5), and it was concluded that CNRc were more representative taking structures that are visually related to each other12. Lenga L et al. agree with this criterion for estimating CNR13 but used a fixed structure to assess noise, reporting variations in contrast-to-noise ratio between different high-resolution diagnostic protocols acquired with various techniques for lung structure between 64.7 and 97.6. Agadakos E et al., report CNRc in lung region for chest studies with significant variation between diagnostic (average effective dose 1.5mSv, range 1.2-2.3mSv) and low dose protocol (average effective dose 0.71 mSv, range 0.7-0.8mSv) from 8.0 (6.7-9.9) and 7.0 (5.4-8.8) respectively, using a fixed background ROI in fat tissue [29]; but the same authors explain that the resulting differences became non-significant when the discrepancies between the two groups of population studies were considered. Steiniger B et al. use similar criteria to calculate CNRc in different abdominal arteries, using a fixed ROI in fat tissue to characterize the noise, reporting values between 3.6 and 89.5 for one patient [30].

There is no apparent significant correlation between the dosimetry parameters CTDIvol and SSDE with the CNRc of the different structures (-0.273<Correlation coefficient <0.03; p<0.05), a situation that perhaps describes the complex dependence between dose, noise, and contrast to noise ratio of the resulting images, also found by other authors [6, 20, 27, 29, 31].

According to Table 3, the CNRca per patient for each protocol ranged from 15.4 to 39.0; while for Diagnostic its minimum was 18.5 and its maximum was 70.5. The differences between both protocols were between -20.2 and 55.1

approximately and were statistically significant (p=0.005), 13/15 patients showed higher values in the diagnostic doses than in the corresponding Low Dose protocol. Patients 4 and 10 showed a decrease in CNRca with the diagnostic protocol. Patient 4 underwent a diagnostic study with different parameters than the rest, so the analysis does not provide valid comparative information. In the case of patient 10, the automatic dose-saving system (DoseRight ACS and X-Z-DOM) generated a significant dose reduction factor producing an exposure of 97mAs, meanwhile, the low-dose system provided 100mAs, resulting in a higher CNRca. This situation shows the sensitivity of this quantitative parameter to variations in the real "exposure and dose" received by the patient. This parameter has only one known bibliographic reference; which reported that CNRca in ROI painted on similar anatomical structures like abdominal arteries was 62.6 % for one patient31, comparable to our results with a CT protocol for high resolution (300 mAs).

Table 4 shows that FWHMc values obtained through the ESF ranged between 0.9 and 2.7mm in the Low Dose protocols, and between 0.7 and 1.7 mm in the Diagnostic protocols. As a trend, the Diagnostic protocols showed lower values, only 2/90 FWHMc had a different behavior. The p-values found during their statistical comparison yielded significant differences for all structures ($p \leq 0.002$). Conversely, the low root means square errors (<0,05) obtained from the fitting function expressed the parameter capabilities to reflect the overall contrast-spatial resolution properties of the clinical image. The FWHMc values obtained through the ESF are higher than those found in the physical phantom by Almahadi (2018) which ranged from 0.1-0.2mm14. However, they were lower than those reported in the initial work developed by this author, where it took values between 0.7-3.5mm 12, probably because of greater variation of clinical protocols, including attenuation correction studies in myocardial perfusion studies (in this only 2 types of protocols were used). In the detailed analysis by structure, it was observed that the range of variation of the estimated FWHMc for the same edge structure showed a significant difference between the two protocols ($p \leq 0.002$). These results confirmed that the anatomical variables make the quality analysis more complex, beyond the spatial resolution and contrast to noise defined in a phantom to specific protocols; with a strong patient-specific character; in a multifactorial way; strengthening the potential of FWHMc as a descriptor metric. Also, table 4 showed that FWHMca per patient for the Low Dose protocol ranged from 1.4 to 1.9mm (SD $\pm$ 0.1) and for the Diagnostic protocol they ranged from 0.9 to 1.2 mm (SD $\pm$ 0.1), finding a significant difference between them(p=0.001). Better mean clinical spatial resolution values were achieved in the high-dose studies (see Figure 2). The correlation between the dosimetry parameter SSDE and the average FWHMca for each study was significant with a Pearson correlation index of -0.63 (p=0.011) in the case of the Low Dose protocol, this implies that the spatial resolution improves to some extent with increasing dose, and does so in a complex and patient-specific manner. This protocol handles fixed mAs, so the discrepancies between patients (Patient Specific Thickness) mark differences between quality parameters such as FWHMca. This situation is not valid for the diagnostic protocol, where there is no correlation with the SSDE (p=0.127), probably a consequence of the dose modulation systems, which vary in a patient-specific way the mAs and the resulting CTDIvol, to sustain the image quality. This hypothesis is supported by the fact that no correlation was found between CNRca and SSDE.

FWHMca using this approach has no known bibliographic references, except for the previous study developed by the author 12. Sanders J. et al, 2016; evaluated MTF on Fourier space using skin/air of clinical image, they found this edge approach was not enough to characterize the spatial resolution properties of the image33. In some cases, when adaptive filtration is used, different edges in the image can be treated differently; showing that one interface would not provide a complete characterization of the image resolution. In this work, it was found a significant correlation between SSDE and FWHMca (Pearson correlation index of -0.45, p = 0.045), showing that in varied protocols the spatial resolution improves to some extent with increasing dose, and does so in a complex and patient-specific manner. Despite the limitations of the short sample size of the study, only 15 patients and one equipment, the particularities shown by these new metrics suggest their further comprehensive study as an integral descriptor of image quality closely related to clinical contrast and spatial resolution, leading to better agreement between subjective and objective quality assessments.

V. CONCLUSIONS

The metrics studied satisfactorily detected differences in image quality between the two protocols, showing the potential to describe important patient image attributes closely related to the detectability of structures and organs. Further work using these metrics should focus on their quantitative value in different scenarios and their relationship to the observer/evaluator.

REFERENCES

[1] United Nations Scientific Committee on the Effects of Atomic Radiation. *UNSCEAR 2020/2021 Report to the General Assembly with Scientific Annex A: Evaluation of Medical Exposure to Ionizing Radiation* (United Nations, New York, 2022). https://www.unscear.org/unscear/uploads/documents/publications/UNSCEAR_2020_21_Annex-A.pdf.

[2] C. J. Martin y M. Barnard. How much should we be concerned about cumulative effective doses in medical imaging? Journal of Radiological Protection **42,** 011514 (ene. de 2022). ISSN: 1361-6498. http://dx.doi.org/10.1088/1361-6498/ac31c1.

[3] G. Frija, J. Damilakis, G. Paulo, R. Loose y E. Vano. Cumulative effective dose from recurrent CT examinations in Europe: proposal for clinical guidance based on an ESR EuroSafe Imaging survey. European Radiology **31,** 5514-5523 (mar. de 2021). ISSN: 1432-1084. http://dx.doi.org/10.1007/s00330-021-07696-1.

[4] I. Sebelego, S. Acho, B. van der Merwe y W. Rae. Size based dependence of patient dose metrics, and image quality metrics for clinical indicator-based imaging protocols

in abdominal CT procedures. Radiography **29,** 961-974 (oct. de 2023). ISSN: 1078-8174. http://dx.doi.org/10.1016/j.radi.2023.07.011.

[5] K. Ohashi, Y. Nagatani, M. Yoshigoe, K. Iwai, K. Tsuchiya, A. Hino, Y. Kida, A. Yamazaki y T. Ishida. Applicability Evaluation of Full-Reference Image Quality Assessment Methods for Computed Tomography Images. Journal of Digital Imaging **36,** 2623-2634 (ago. de 2023). ISSN: 1618-727X. http://dx.doi.org/10.1007/s10278-023-00875-0.

[6] P. Barca, F. Paolicchi, G. Aringhieri, F. Palmas, D. Marfisi, M. E. Fantacci, D. Caramella y M. Giannelli. A comprehensive assessment of physical image quality of five different scanners for head CT imaging as clinically used at a single hospital centre—A phantom study. PLOS ONE **16** (ed. Pratx, G.) e0245374 (ene. de 2021). ISSN: 1932-6203. http://dx.doi.org/10.1371/journal.pone.0245374.

[7] E. J. I. Hoeijmakers, B. Martens, B. M. F. Hendriks, C. Mihl, R. L. Miclea, W. H. Backes, J. E. Wildberger, F. M. Zijta, H. A. Gietema, P. J. Nelemans y C. R. L. P. N. Jeukens. How subjective CT image quality assessment becomes surprisingly reliable: pairwise comparisons instead of Likert scale. European Radiology **34,** 4494-4503 (ene. de 2024). ISSN: 1432-1084. http://dx.doi.org/10.1007/s00330-023-10493-7.

[8] W. Lee, E. Cho, W. Kim, H. Choi, K. S. Beck, H. J. Yoon, J. Baek y J.-H. Choi. No-reference perceptual CT image quality assessment based on a self-supervised learning framework. Machine Learning: Science and Technology **3,** 045033 (dic. de 2022).

[9] International Atomic Energy Agency. *Patient Radiation Exposure Monitoring in Medical Imaging* 112 (International Atomic Energy Agency, Vienna, Austria, 2023). https://www.iaea.org/publications/15202/patient-radiation-exposure-monitoring-in-medical-imaging.

[10] S. L. Brady. Implementation of AI image reconstruction in CT—how is it validated and what dose reductions can be achieved. The British Journal of Radiology **96** (abr. de 2023). ISSN: 1748-880X. http://dx.doi.org/10.1259/bjr.20220915.

[11] H. Jiang, S. Qin, L. Jia, Z. Wei, W. Xiong, W. Xu, W. Gong, W. Zhang y L. Yu. Deep learning based ultra-low dose fan-beam computed tomography image enhancement algorithm: Feasibility study in image quality for radiotherapy. Journal of Applied Clinical Medical Physics **25** (nov. de 2024). ISSN: 1526-9914. http://dx.doi.org/10.1002/acm2.14560.

[12] A. L. Díaz, D. D. R. Rosales, R. N. M. Álvarez, J. R. Garrido, J. M. M. Escuela y A. del Pozo Almaguer. CT image quality metrics implementation during thorax SPECT/CT clinic studies. Revista Brasileira de Física Médica **17,** 724 (jul. de 2023). ISSN: 2176-8978. http://dx.doi.org/10.29384/rbfm.2023.v17.19849001724.

[13] L. Lenga, D. Leithner, J. L. Peterke, M. H. Albrecht, T. Gudauskas, T. D'Angelo, C. Booz, R. Hammerstingl, T. J. Vogl, S. S. Martin y J. L. Wichmann. Comparison of Radiation Dose and Image Quality of Contrast-Enhanced Dual-Source CT of the Chest: Single-Versus Dual-Energy and Second-Versus Third-Generation Technology. American Journal of Roentgenology **212,** 741-747 (abr. de 2019). ISSN: 1546-3141. http://dx.doi.org/10.2214/AJR.18.20065.

[14] A. M. Alshweikh, K. Kusminarto y G. B. Suparta. An Improved Method of Measuring Spatial Resolution of the Computed Tomography from ESF based on CT phantom images. International Journal of Applied Engineering Research **13,** 12318-12325 (2018). ISSN: 0973-4562. https://api.semanticscholar.org/CorpusID:174785359.

[15] T. Otzen, C. Manterola, M. Mora, G. Quiroz, P. Salazar y N. García. Statements, Recommendations, Proposals, Guidelines, Checklists and Scales Available for Reporting Results in Biomedical Research and Quality of Conduct: A Systematic Review. International Journal of Morphology **38,** 774-786 (2020). https://intjmorphol.com/wp-content/uploads/2020/03/art_38_383-.pdf.

[16] Philips Healthcare. *Manual del Usuario PET/CT Philips Gemini 64TF* Philips Healthcare (abr. de 2012). https://www.philips.ie/healthcare/product/HC889474/diamond-select-gemini-tf-64--pet-ct-scanner.

[17] A. López, A. del Pozo, A. Machado, K. Batista, C. F. Calderón y L. A. Torres. Calidad de la imagen de tomografía computarizada versus dosis en estudios híbridos: resultados preliminares en maniquí. Medisur **20,** 272-284 (2022). http://medisur.sld.cu/index.php/medisur/article/view/5409.

[18] C. Ubeda de la C., E. Vaño C., R. Ruiz Cruces., P. Soffia S. y D. Fabri G. Niveles de referencia para diagnóstico: Una herramienta efectiva para la protección radiológica de pacientes. Revista chilena de radiología **25,** 19-25 (mar. de 2019). ISSN: 0717-9308. http://dx.doi.org/10.4067/S0717-93082019000100019.

[19] J. Boone, K. Strauss y D. Cody. Size-specific dose estimates (SSDE) in pediatric and adult body CT examinations. College Park (MD): American Association of Physicists in Medicine (AAPM) (ene. de 2011).

[20] F. Verdun, D. Racine, J. Ott, M. Tapiovaara, P. Toroi, F. Bochud, W. Veldkamp, A. Schegerer, R. Bouwman, I. H. Giron, N. Marshall y S. Edyvean. Image quality in CT: From physical measurements to model observers. Physica Medica **31,** 823-843 (dic. de 2015). ISSN: 1120-1797. http://dx.doi.org/10.1016/j.ejmp.2015.08.007.

[21] M. Ponnusamy, D. Halanaik y V. Rajaraman. Size specific dose estimate (SSDE) for estimating patient dose from CT used in myocardial perfusion SPECT/CT. Asia Oceania Journal of Nuclear Medicine and Biology (oct. de 2019). https://doi.org/10.22038/aojnmb.2019.40863.1276.

[22] K. M. Kanal, P. F. Butler, D. Sengupta, M. Bhargavan-Chatfield, L. P. Coombs y R. L. Morin. U.S. Diagnostic Reference Levels and Achievable Doses for 10 Adult CT Examinations. Radiology **284,** 120-133 (jul. de 2017). ISSN: 1527-1315. http://dx.doi.org/10.1148/radiol.2017161911.

[23] K. Abe, M. Hosono, T. Igarashi, T. Iimori, M. Ishiguro, T. Ito, T. Nagahata, H. Tsushima y H. Watanabe. The 2020 national diagnostic reference levels for nuclear medicine in Japan. Annals of Nuclear Medicine **34,** 799-806 (ago. de 2020). ISSN: 1864-6433. http://dx.doi.org/10.1007/s12149-020-01512-4.

[24] Health Information and Quality Authority. *Diagnostic Reference Levels: Guidance on the Establishment, Use and Review of Diagnostic Reference Levels for Medical Exposure to Ionising Radiation* HIQA Guidance Document (Health Information y Quality Authority, Dublin, Ireland, 2023). https://www.hiqa.ie/sites/default/files/2023-07/Diagnostic-Reference-Levels-Guidance.pdf (2024).

[25] V. Chatzaraki, R. A. Kubik-Huch, M. Thali y T. Niemann. Quantifying image quality in chest computed tomography angiography: Evaluation of different contrast-to-noise ratio measurement methods. Acta Radiologica **63,** 1353-1362 (oct. de 2021). ISSN: 1600-0455. http://dx.doi.org/10.1177/02841851211041813.

[26] D. Ippolito, C. Talei Franzesi, C. Cangiotti, L. Riva, A. De Vito, D. Gandola, C. Maino, P. Marra, G. Muscogiuri y S. Sironi. Inter-observer agreement and image quality of model-based algorithm applied to the Coronary Artery Disease-Reporting and Data System score. Insights into Imaging **13** (nov. de 2022). ISSN: 1869-4101. http://dx.doi.org/10.1186/s13244-022-01286-5.

[27] Y. M. Wong, C. C. Ong, C. R. Liang, C. A. Tan y L. L. S. Teo. Image quality, contrast enhancement and radiation dose of electrocardiograph- versus non-electrocardiograph-triggered computed tomography angiography of the aorta. Singapore Medical Journal **65,** 84-90 (oct. de 2021). ISSN: 2737-5935. http://dx.doi.org/10.11622/smedj.2021166.

[28] B. Kataria, J. Nilsson Althén, Ö. Smedby, A. Persson, H. Sökjer y M. Sandborg. Assessment of image quality in abdominal computed tomography: Effect of model-based iterative reconstruction, multi-planar reconstruction and slice thickness on potential dose reduction. European Journal of Radiology **122,** 108703 (ene. de 2020). ISSN: 0720-048X. http://dx.doi.org/10.1016/j.ejrad.2019.108703.

[29] E. Agadakos, A. Zormpala, N. Zaios, C. Kapsiocha, M. N. Gamaletsou, M. Voulgarelis, N. V. Sipsas, L. A. Moulopoulos y V. Koutoulidis. The Use of Low-Dose Chest Computed Tomography for the Diagnosis and Monitoring of Pulmonary Infections in Patients with Hematologic Malignancies. Cancers **16,** 186 (dic. de 2023). ISSN: 2072-6694. http://dx.doi.org/10.3390/cancers16010186.

[30] B. Steiniger, M. Fiebich, M.-O. Grimm, A. Malouhi, J. R. Reichenbach, M. Scheithauer, U. Teichgräber y T. Franiel. PAE planning: Radiation exposure and image quality of CT and CBCT. European Journal of Radiology **172,** 111329 (mar. de 2024). ISSN: 0720-048X. http://dx.doi.org/10.1016/j.ejrad.2024.111329.

[31] N. F. Ukaji, C. C. Ohagwu y M. P. Ogolodom. Effects of Variations in Imaging Parameters on Image Quality of Non Contrast Computed Tomography Scans of Brain: A Cross-sectional Study. JOURNAL OF CLINICAL AND DIAGNOSTIC RESEARCH (2021). ISSN: 2249-782X. http://dx.doi.org/10.7860/JCDR/2021/49791.15527.